ACS OMEGA

Article

Cite This: ACS Omega 2019, 4, 4040−4048

http://pubs.acs.org/journal/acsodf

Sustained Releasing of Methotrexate from Injectable and Thermosensitive Chitosan−Carbon Nanotube Hybrid Hydrogels Effectively Controls Tumor Cell Growth

Leyla Saeednia,*[,†,∥] Li Yao,[‡] Kim Cluff,[§] and Ramazan Asmatulu[†]

[†]Department of Mechanical Engineering, Wichita State University, 1845 Fairmount Street, Wichita, Kansas 67260-0133, United States

[‡]Department of Biological Sciences, Wichita State University, 1845 Fairmount Street, Wichita, Kansas 67260-0133-0026, United States

[§]Department of Biomedical Engineering, Wichita State University, 1845 Fairmount Street, Wichita, Kansas 67260-0066, United States

ABSTRACT: Injectable thermosensitive hydrogels have been widely investigated for drug delivery systems. Chitosan (CH) is one of the most abundant natural polymers, and its biocompatibility and biodegradability make it a favorable polymer for thermosensitive hydrogel formation. The addition of nanoparticles can improve its drug release behavior, remote actuation capability, and biological interactions. Carbon nanotubes (CNTs) have been studied for the use in drug delivery systems, and they can act as drug delivery vehicles to improve the delivery of different types of therapeutic agents. In this work, carbon nanotubes were incorporated into a thermosensitive and injectable hydrogel formed by chitosan and β-glycerophosphate (β-GP) (CH−β-GP−CNTs). The hybrid hydrogels loaded with methotrexate (MTX) were liquid at room temperature and became a solidified gel at body temperature. A number of tests including scanning electron microscopy, Fourier transform infrared spectroscopy, Raman spectroscopy, and X-ray diffraction were utilized to characterize the MTX-loaded CH−β-GP−CNT hybrid hydrogels. The cell viability (alamarBlue) assay showed that hydrogels containing CNT (0.1%) were not toxic to the 3T3 cells. In vitro MTX release study revealed that CNT-containing hydrogels (with 0.1% CNT) demonstrated a decreased MTX releasing rate compared with control hydrogels without CNT. The cultured MCF-7 breast cancer cells were used to evaluate the efficacy of CH−β-GP−CNT hybrid hydrogels delivering MTX on the control of tumor cell growth. Results demonstrated that CNT (0.1%) in the hydrogel enhanced the MTX antitumor function. Our study indicates that a thermosensitive CH−β-GP−CNT hybrid hydrogel can be used as a potential breast cancer therapy system for controlled delivery of MTX.

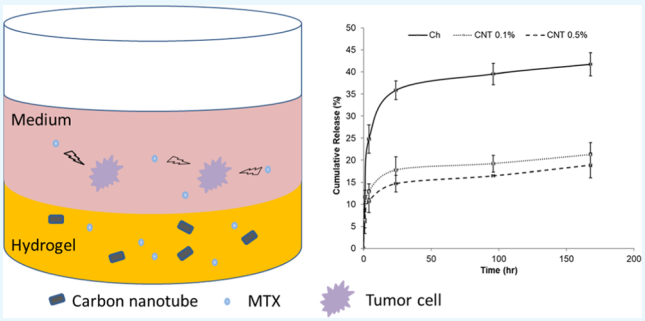

1. INTRODUCTION

Breast cancer can be treated if diagnosed in the early stages. Among the different methods of cancer treatment, chemotherapy is the most commonly used and up-to-date approach. Moreover, chemotherapy is an essential step before and after surgery to treat the tumor and prevent reoccurrence and metastasis.[1,2] However, the toxicity generated by chemotherapeutic agents is a major concern of chemotherapy. The effect of therapeutic agents administrated intravenously is nonspecific in nature since they generate function on both diseased and healthy cells, consequently causing undesired side effects. To generate a more efficient therapeutic effect, efforts have made in the past decade to develop a targeted drug delivery system.[3]

Among the different materials used for drug delivery applications, polymeric hydrogels have attracted major attention.[4,5] Hydrogels are defined as cross-linked polymeric networks that have the ability to absorb an enormous amount of water or biological fluid, despite the fact that they are actually insoluble in water.[6] Hydrogels can be made of natural polymers such as chitosan (CH), gelatin, collagen, and dextran. Biocompatibility and biodegradability of natural polymers make them suitable for biomedical applications, especially as drug delivery devices.[7] In situ forming hydrogels have the ability to respond to environmental stimuli such as temperature, pressure, light, pH, ions, and molecules as well as electric, magnetic, and sound fields.[8]

As one type of biopolymers, chitosan has been investigated as implantable biomaterials.[7,9,10] Studies have shown that the chitosan-based scaffolds are highly biocompatible.[11−13] The β-

Received: November 18, 2018
Accepted: February 12, 2019
Published: February 22, 2019

DOI: 10.1021/acsomega.8b03212
ACS Omega 2019, 4, 4040−4048

glycerophosphate (β-GP) can function as a neutralizing agent to facilitate the chitosan to form a thermosensitive hydrogel. Because the mixture of chitosan and β-GP can form a hydrogel at body temperature (37 °C), they can potentially be used as injectable biomaterials for drug delivery.[14−16]

The main drawback of the CH−β-GP hydrogels is their lack of mechanical strength, which can be improved by incorporating nanoparticles, thus improving their drug release behavior and biological interactions.[17] Hydrogel hybrids with nanoparticle inclusions, such as clay, gold, silver, iron oxide, and carbon nanotubes (CNTs), have been synthesized and studied for possible biomedical applications.[18]

Several research studies have focused on CNT usage in biological systems. CNTs have been shown to be a potential scaffold material in nanobiotechnology applications. Moreover, they have been studied for drug delivery systems, and it has been found that the delivery of different types of therapeutic agents improves by using CNTs as the drug delivery vehicle. The main reason for the effectiveness of CNTs in drug delivery applications is their high surface area, which allows for a high loading capacity of therapeutic drugs.[19−22] The biocompatibility of CNTs depends on a number of factors including their fabrication process, the presence of impurities (normally metallic catalysts), their size and shape, their dispersion and aggregation station as well as the method of administration and cellular uptake.[23,24]

Several polysaccharides with CNT incorporation have been studied to investigate the effect of this addition on hydrophilicity/hydrophobicity and surface chemistry on cell behavior.[25] In one study, CH hydrogel beads were prepared using different amounts of CNTs, and their mechanical strength, acid stability, and adsorption capacity to an anionic dye were examined.[26] Gelatin, which has also been used to synthesize CNT hybrid hydrogels, is another prospective material in biomedical applications. The swelling (SW) property of physically mixed gelatin/CNT hydrogels was examined in one of the earliest studies in this field.[27] In another study, gellan gum (water soluble anionic polysaccharide) was incorporated with CNTs to make an electrically conductive hydrogel for the purpose of electrical cell stimulation. Results showed that 1.3 wt % of CNT was required to achieve an electrically conductive hydrogel for the stated purpose.[28] Carbon nanotubes and carbon nanofibers were used to reinforce poly(vinyl alcohol) (PVA) hydrogels for an osteochondral repair, and this combination showed better biological responses than pure PVA hydrogels.[29] In another study, CNT−PVA hybrid hydrogels were prepared and investigated for their swelling and mechanical properties.[20] The addition of multiwalled carbon nanotubes (MWNTs) was studied in freeze-dried chitosan scaffolds in a 2012 study by Venkatesan et al.,[30] who suggested that CH−MWNTs scaffolds have a potential use in bone tissue engineering. In one of the latest studies, in 2014, Aryaei et al.[31] investigated the mechanical and biological properties of CH−CNT nanocomposite films. They concluded that the tensile strength and elastic modulus were improved by adding 1 wt % of MWNTs to the chitosan matrix. Also, in their study, no cell toxicity was observed after 3 and 7 days of cell proliferation tests on CH−MWNT nanocomposites.

In this study, we fabricated a CH−β-GP−CNTs hydrogel by incorporating CNTs into the CH−β-GP. We characterized the hydrogels using scanning electron microscopy (SEM), Fourier transform infrared (FTIR) spectroscopy, X-ray diffraction (XRD), and Raman spectroscopy. The releasing profile of methotrexate (MTX) from CH−β-GP−CNTs hydrogels was analyzed. The MTX-loaded chitosan hydrogels have been tested for its function on the control of MCF-7 breast cancer cell growth. We demonstrated that the nanohybrid hydrogels significantly improved antitumor function of MTX in vitro test.

2. RESULTS AND DISCUSSION

2.1. Structural Analysis. The hydrogels were formed after incubation of the solution in an incubator of 37 °C. Figure 1

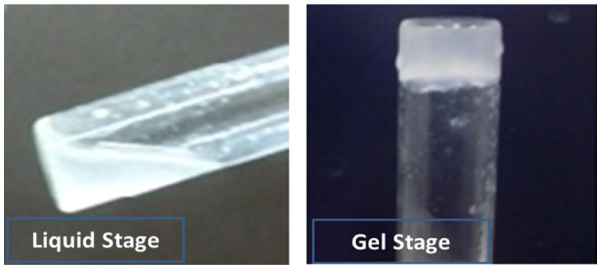

Figure 1. Chitosan/β-GP at room temperature (left) and 37 °C (right).

shows the chitosan/β-GP at room temperature (left) and 37 °C (right). Figure 2A−F shows SEM images of CH−β-GP−CNT hydrogels. All hydrogels indicated an irregular porous structure. It can be seen that the blank CH−β-GP hydrogel shows a porous structure (Figure 2A) with a fairly smooth matrix surface (Figure 2B); whereas by the addition of CNT (0.1 and 0.5%), the hydrogels' appearance look falking (Figure 2C,E), and the surface roughness seems to increase (Figure 2D,F). The surface roughness can be attributed to the agglomerations of CNTs within the polymeric matrix. However, CH−β-GP−CNT nanohybrid hydrogels still presented as a structure with small porosity. Therefore, it can be concluded that the fabricated CH−β-GP−CNT hydrogels are suitable for various biomedical applications, such as tissue implants as well as drug delivery systems porosity.[32−34]

Contact angle measurements were made using water as the liquid phase, since the density of water (1 g/cm^3) is similar to the density of the extracellular fluid within the body, which is mainly blood (1.06 g/cm^3). The work of adhesion, which is the energy required for two surfaces to adhere to each other, is a rough estimation of the surface energy. The results for contact angle and work of adhesion for different hydrogel samples are shown in Table 1.

From Table 1, it can be seen that the addition of nanoparticles increases the contact angle and hydrophobicity. It has been reported that hydrophobic materials are desirable options for drug delivery applications, since hydrophobicity decreases the degradation kinetics and lowers the drug release behavior as well.[35] Moreover, cell adhesion and biocompatibility were found to be maximized on surfaces with water contact angles of 60−90°.[36] The work of adhesion decreases with increasing nanotube concentration. Surface adhesion and contact angle are dependent on a variety of factors, such as the presence of chemical bonding, impurities, surface roughness, oxide layer, etc. Therefore, an accurate conclusion is complicated because of the interaction of different factors. However, the test results are consistent with the literature. All three carbon-based nanomaterials used in this work were shown to increase surface hydrophobicity.[37−39]

DOI: 10.1021/acsomega.8b03212
ACS Omega 2019, 4, 4040−4048

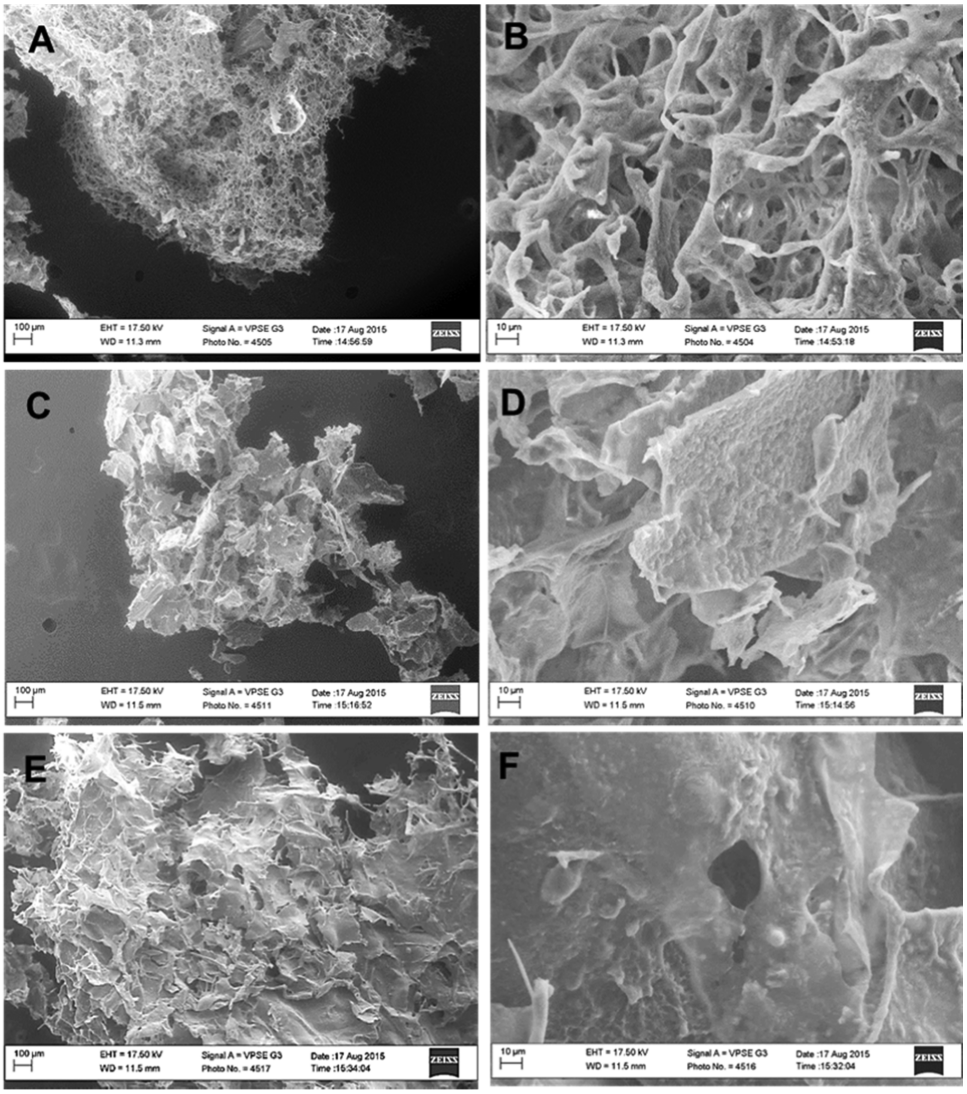

Figure 2. SEM imaging of freeze-dried hydrogels. (A, B) CH−β-GP hydrogel, (C, D) CH−β-GP−CNT (0.1%) hybrid hydrogel, and (E, F) CH−β-GP−CNT (0.5%) hybrid hydrogel. The control (a) and (b) are reproduced from Saeednia et al. with permission from John Wiley and Sons.

Table 1. Contact Angles and Work of Adhesion of Hybrid Hydrogels

sample	contact angle (°)	work of adhesion (mJ/m^2)
chitosan	82 ± 1	8.14
CH−CNT 0.1%	85 ± 2	7.80
CH−CNT 0.5%	89 ± 2	7.23

FTIR spectra results are shown in Figure 3A,B. The spectra of CH−CNT (0, 0.1, and 0.5% of CNT) hydrogels are also provided in Figure 3A. The characteristic peaks of chitosan (as in Figure 3B) can be observed in all of the hydrogels' spectra. The C−O stretching at 1050 and 970 cm^{-1} indicates the characteristic saccharide structure of chitosan. The C−CH_3 symmetric deformation appeared at around 1420 cm^{-1}. A wide peak variation in the range of 3750−3000 cm^{-1} is due to stretching vibrations of the OH groups, which are overlapped with the stretching vibrations of N−H. The two small peaks at 2870 and 2890 cm^{-1} are attributed to C−H bonding in the −CH_2 and C−H_3 groups, respectively. Peaks in the range of 1680−1480 cm^{-1} are assigned to amide and amine groups, where carbonyl bond (C═O) vibrations of the secondary amide group are at 1645 cm^{-1}, and protonated amine group NH_3 vibrations are at 1584 cm^{-1}. β-GP characteristic peaks (Figure 3B) were also recognizable in the CH−β-GP hybrid hydrogel spectra. The peak at 3233 cm^{-1} is due to hydrogen-bonded O−H stretching. Typical bands of the inorganic phase for the PO43 groups are shown as the mode at 900−1200 cm^{-1}. With the addition of CNTs, a slight variation in stretching frequency was observed, which can be attributed to pi-bonds of the carbon nanotube chemically interacting with the amide and OH groups of the chitosan. However, most peaks belong to CH moieties, therefore we can conclude that there was no chemical bonding formation between chitosan and CNT.[30,31,40]

Raman spectrum tests were performed for pure CNT and the hybrid hydrogel containing 0.5% of CNT (Figure 3C). Raman spectrum test can characterize the molecular morphology of carbon nanomaterials. The tests of Raman spectra and FTIR provide a better understanding of how nanotubes change the chemical structure of hydrogels. In both CNT and CH−CNT spectra, the characteristic D-band and G-band peaks are visible at 1330 and 1580 cm^{-1}, respectively. The Raman spectrum of a CNT is similar to graphene, which is

DOI: 10.1021/acsomega.8b03212
ACS Omega 2019, 4, 4040−4048

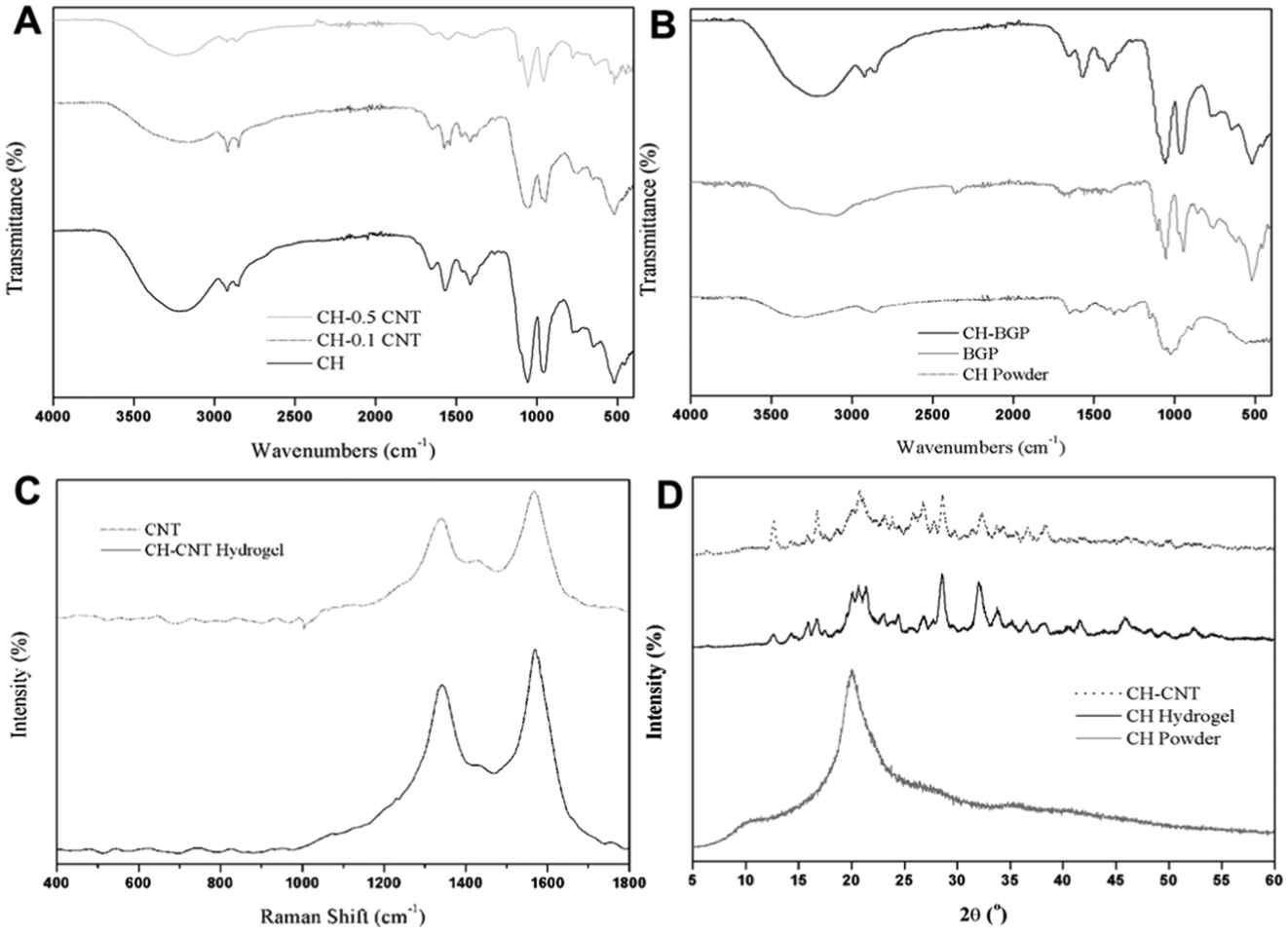

Figure 3. Characterization of hydrogels. (A) FTIR spectra of CH−CNT (0, 0.1, and 0.5%) hybrid hydrogels. (B) FTIR spectra of CH powder, β-GP powder, and CH−β-GP hydrogel. (C) Raman spectra of CNT and CH−CNT 0.5% hybrid hydrogel. (D) XRD patterns of CH powder, CH hydrogel, and CH−CNT hybrid hydrogel.

not too surprising since a CNT is composed of rolled-up sheets of graphene.[41] Since the intensities of the CNT peaks are much higher than the intensity of chitosan peaks, none of the chitosan peaks was observed. Overall, Raman spectroscopy confirmed the presence of nanotubes in the hybrid hydrogels and showed no changes in the chemical structure of nanoparticles.[31,42−45]

Figure 3D shows the results of XRD analysis. Currently, six polymorphs of chitosan are known. Normally, chitosan shows three XRD peaks, corresponding to two different crystalline structures. The hydrated (tendon) crystalline structure shows a peak at $2\theta = 10°$ (or two peaks at $2\theta = 8$ and 12°), whereas the anhydrous crystalline structure shows one peak at $2\theta = 15°$. Chitosan also shows a broad peak around $2\theta = 20°$, which is due to the existence of an amorphous structure. The XRD pattern of chitosan powder (Figure 3D) shows that the chitosan used in this study had a hydrated (tendon) crystalline structure.

Chitosan is a semicrystalline polymer, whereas β-glycerophosphate is a crystalline solid. The XRD pattern of the CH hydrogel shows the characteristic peaks of chitosan. From the XRD graph of CH−CNT, it can be seen that the incorporation of CNTs into the CH hydrogel did not affect the crystalline structure of chitosan, since there was no significant change in the XRD pattern of the CH−CNT hybrid hydrogel in comparison with the pure chitosan hydrogel. The addition of 0.5% CNTs to the chitosan hydrogel did not seem to make a noticeable change in the XRD pattern. However, a graphite-like peak (002) at 25.78° is present, which is the main characteristic peak of CNTs.[43] These results are consistent with those in the literature.[30,31,46−48]

2.2. Swelling and Degradation Behavior of Hydrogels. The swelling (SW) profile of CH−β-GP−CNT hydrogels was tested. The hydrogel samples were incubated in phosphate buffer solution (PBS) at 37 °C, and then the sample weight was measured at various time points. The results showed that the addition of carbon nanotubes in the hydrogels increased the sample swelling ratio (Figure 4). The swelling kinetics of the hydrogels was analyzed according to the following equation. The amount of water absorbed by a hydrogel at a specific time (t) is shown as M_t, which is equal to $W_t - W_0$. In the equation, k represents the swelling characteristic constant and n is the diffusional exponent. Both k and n depend on the polymer−solvent system. The swelling ratio (water uptake) was calculated as M_t/W_0, which is an exponential function of time

$$\mathrm{SW} = \frac{M_t}{W_0} = kt^n$$

Two types of swelling processes can be considered according to the equation: the Fickian or diffusion-controlled swelling process and the non-Fickian swelling process. In Fickian

DOI: 10.1021/acsomega.8b03212
ACS Omega 2019, 4, 4040−4048

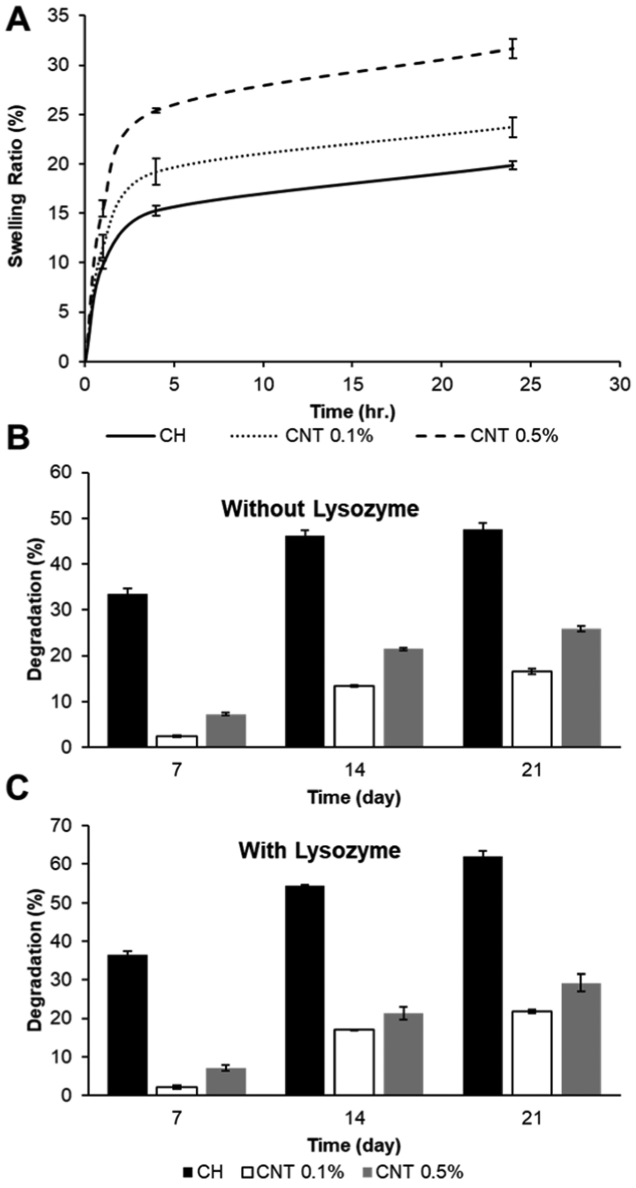

Figure 4. Swelling and degradation analysis of hydrogels. (A) Swelling ratios of CH−β-GP−CNT (0, 0.1, and 0.5%) hybrid hydrogel. (B, C) Degradation assay of CH−β-GP−CNT (0, 0.1, and 0.5%) hybrid hydrogels.

swelling process ($n \leq 0.5$), the solvent diffusion rate is slower than the relaxation rate of the polymer chain. There are two types of non-Fickian swelling processes which are relaxation-controlled, when the diffusion rate is higher than that of relaxation ($n = 1$) and anomalous diffusion, when the diffusion and relaxation rates are comparable ($0.5 < n < 1$). When the logarithmic values of SW versus time are plotted, the slope of the plot is indicated as n and the intercept value is indicated as k. Because the n values of the tested hydrogels were ≤ 0.5 (results not shown) in this study, we conclude that the swelling behavior of chitosan hydrogels with and without nanotubes fits the Fickian process.[49−53]

Hydrogel degradation has been known to have a vital impact on drug release behavior. The degradation profile of the hybrid chitosan hydrogels is tested in this study (Figure 4B,C). We show that the addition of lysozyme amplified the hydrogel degradation rate as reported.[54] Also, the inclusion of carbon nanotubes showed a decrease in weight loss. Although chitosan hydrogels in the presence of lysozyme degraded about 61.9% in 3 weeks, the CNT-loaded chitosan hydrogels had degradation values of 16.5 and 25.9% for 0.1 and 0.5% CNT inclusions, respectively. These results confirm that the interactions between chitosan and CNTs improve the biological properties.

2.3. Cell Viability Assay. The toxicity of prepared hydrogels was studied using the alamarBlue reagent.[55] The fibroblast 3T3 cells were grown on top of the hydrogels for 4 days; cell viability percentage results are shown in Figure 5A. Addition of carbon nanotubes did not stop cell growth, and compared to the control, which is the CH−β-GP hydrogel without any CNT cells, it can be seen that cells are still growing on top of the CH−β-GP−CNT hydrogel. However, the addition of carbon nanotubes decreases cell growth to some point comparable to the pure chitosan hydrogel, yet the cell viability is still more than 80%, which is acceptable in biomedical applications. These results confirm that the fabricated hydrogel in this study is biocompatible. The fluorescent imaging assay of cytoskeleton was carried out to confirm the cell viability. The fixed 3T3 cells were labeled with rhodamine phalloidin (red) and Hoechst (blue). The cell morphology in taken images (Figure 5B−D) clearly demonstrated the live cells and confirmed the viability of 3T3 cells after culturing on hydrogels for 4 days. The study showed that the hydrogel containing 0.1% CNT should be an optimal condition for drug delivery. The test is also consistent with alamarBlue results that increasing of CNT amount in hydrogels decreased the cell viability.[31]

2.4. In Vitro Methotrexate Release. The cumulative methotrexate (MTX) release from CH−β-GP−CNT hybrid hydrogels for 7 days in vitro is shown in Figure 6. The incorporation of CNTs in the hydrogels reduced the initial burst release of MTX. The amount of released MTX from the hydrogel without CNT was 24.7% in the first 4 h, whereas hydrogels with 0.1 and 0.5% of CNT decreased the MTX release to 12.9 and 10.7%, respectively. By increasing the concentration of CNTs, the burst release decreased. Then, the release rate decreased after 24 h. The nanoparticle-loaded hydrogels and control hydrogels basically showed a similar releasing trend after 24 h. This trend may be caused by the following mechanism. First, the MTX that is partially absorbed onto the surface of the hydrogels during gelation results in the initial burst release. The MTX in the gel matrix can show a decreased releasing rate. Second, the decrease in the MTX concentration gradient (dC/dx) can also cause a decreased MTX releasing over time. The addition of CNTs in the hydrogel matrix resulted in an extensive bonding that causes a rigid network. The diffusion of MTX from a rigid network is slower than that from a loose network. The reduction of the amount of burst release is desired for drug therapeutic function since it allows the therapeutic drug to maintain an optimal level for a prolonged therapeutic period of time.[13,56]

To understand the in vitro releasing kinetics (or pharmacokinetics) of MTX from the CNT-loaded hydrogels and control hydrogels, the drug release profile was fitted into the Korsmeyer−Peppas model

$$\frac{M_t}{M_\infty} = K^* t^n$$

DOI: 10.1021/acsomega.8b03212
ACS Omega 2019, 4, 4040−4048

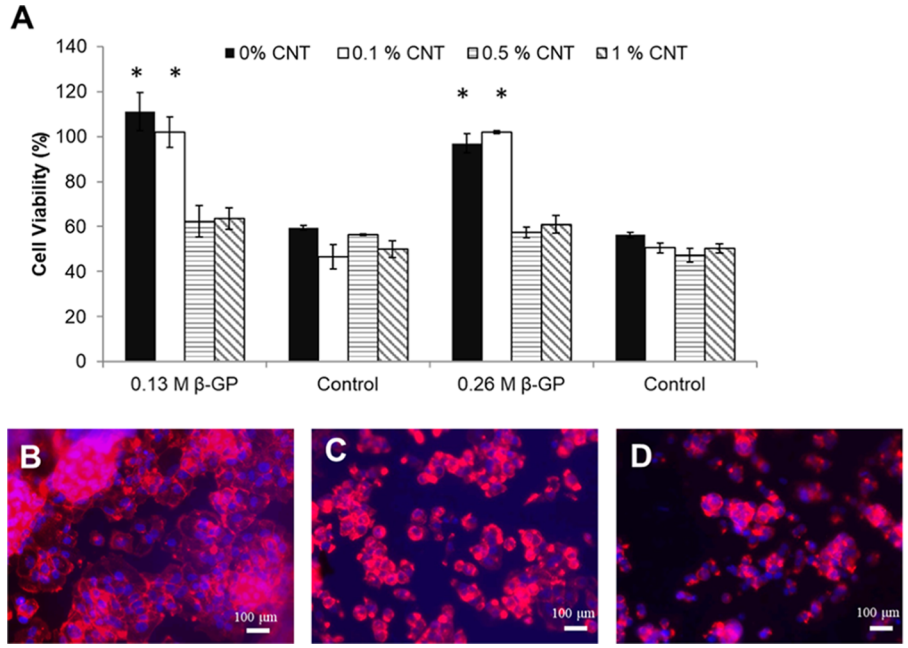

Figure 5. Cell viability assay and cell morphology of cells grown on hydrogels. (A) Cell viability of 3T3 cells grown on CH−β-GP−CNT hybrid hydrogels. (B−D) Fluorescence microscopic images of 3T3 cells labeled with the rhodamine phalloidin and Hoechst. (B) CH−β-GP hydrogel, (C) CH−β-GP−CNT 0.1% hybrid hydrogel, and (D) CH−β-GP−CNT 0.5% hybrid hydrogel. *p < 0.05, compared with the groups of hydrogels containing 0.5% CNT and 1% CNT.

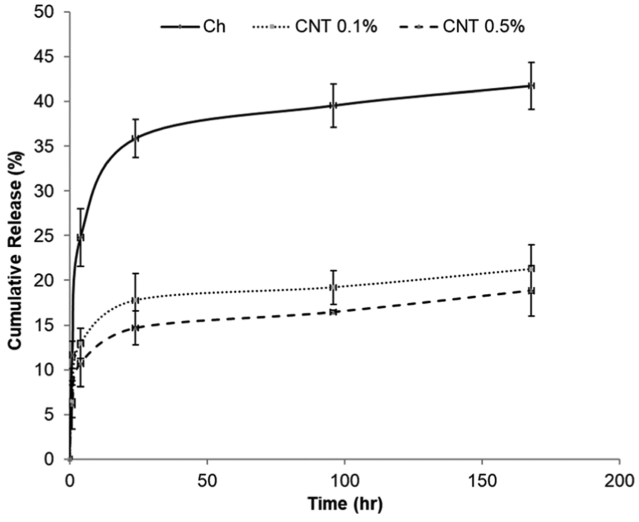

Figure 6. Release of methotrexate from CH−β-GP−CNT hybrid hydrogels.

In the equation, M_t and M_∞ represent the fraction of drug release at time t, and K represents the release rate constant. The n represents the release exponent. The model was analyzed using the solver tool in Excel 2013 (Microsoft Corporation, Redmond, WA). The release rate constant (K), release exponent (n), and the correlation coefficient are calculated and reported in Table 2.

In 1983, Korsmeyer et al.[57] described the drug release from a polymeric system using a simple model, which is now known as the Korsmeyer−Peppas model. This model fits well for cylindrical shaped matrices, and the mechanism of drug release is characterized by the value of the release exponent (n). The releasing mechanism is through the Fickian diffusion when n is ≤0.45. However, it indicates the non-Fickian transport when n is between 0.45 and 0.89.[49] All of these assumptions are consistent with our drug delivery system. Therefore, the obtained n values from this study (Table 2) suggested that the MTX releasing from all of the chitosan hybrid hydrogels had the Fickian diffusion behavior, and the loaded CNT in the hydrogels did not change the drug release mechanism.

Table 2. Releasing Rate Constant (k) and Correlation Coefficient (R^2) for CH−β-GP−CNT Hybrid Hydrogels

sample	K	n	R^2
chitosan	17.3	0.18	0.998656
CH−CNT 0.1%	9.0	0.17	0.999709
CH−CNT 0.5%	7.6	0.17	0.999873

2.5. In Vitro Antitumor Activity. The almarBlue assay viability assay was used to determine the antiproliferative effect of MTX-loaded CH−β-GP−CNT hydrogels on the cultured MCF-7 breast cancer cells. The cell viability was reported as the percent reduction of the almarBlue agent. The cell viability of MCF-7 cells was tested after they were grown on MTX-loaded hydrogels for 4 days (Figure 7). First, the study shows that the addition of CNTs (0.1%) in the CH−β-GP hydrogel did not change the cell viability, but the higher concentration of CNTs (0.5%) reduced cell proliferation significantly. This result indicated the toxicity of CNT at a high concentration (0.5%) in the hydrogel. Second, the antitumor effect of MTX is clearly demonstrated. The MTX in both CH−β-GP−CNT hydrogel and CH−β-GP hydrogel significantly reduced tumor cell (MCF-7) viability compared with the corresponding hydrogels without MTX. Third, the study demonstrated that the addition of CNT (0.1%) in the hydrogel enhanced MTX antitumor effect.

In the MTX releasing study, we characterized the MTX releasing profile and found that the CNT component in the CH−β-GP−CNT hydrogel reduced the MTX releasing rate (Figure 5). The cumulative amount of the released MTX from

DOI: 10.1021/acsomega.8b03212
ACS Omega 2019, 4, 4040−4048

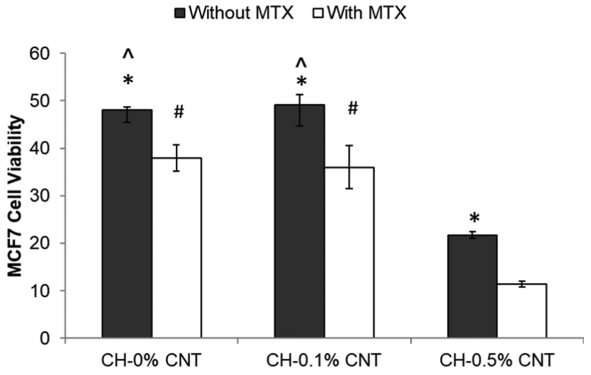

Figure 7. Antitumor efficacy of MTX-loaded CH−β-GP−CNT hybrid hydrogels. $^{*}p < 0.05$, compared with the group treated with MTX. $^{\wedge}p < 0.05$, compared with the CH-0.5% CNT group. $^{\#}p < 0.05$, compared with the CH-0.5% CNT group.

CH−β-GP−CNT hydrogel (with 0.1% CNT) at the time point of 96 h (4 days) was 50% less than that released from CH−β-GP hydrogel. However, the MTX-loaded CH−β-GP−CNT hydrogel (with 0.1% CNT) and MTX-loaded CH−β-GP hydrogel showed a similar effect on reducing cell viability of tumor cells (MCF-7) grown on those hydrogels. The study suggests that CNT enhanced MTX function with a low level of MTX in the cell cultured medium because of its slow releasing rate from CH−β-GP−CNT hydrogel. Also, sharp edges of CNTs may cause cancerous cell membrane damages and leak out the cells, thus shrinking the tumor size. Therefore, the incorporation of CNTs in the MTX-loaded hydrogels can significantly inhibit cancer cell growth with less toxicity to normal cells. These observations are consistent with the investigation of the effect of released MTX on cell viability in a previous report.[12]

3. CONCLUSIONS

In summary, we successfully fabricated thermosensitive chitosan−carbon nanotube hybrid hydrogels. We show analyzed the surface morphology using SEM and found that increase of the nanotube concentration in the hydrogels increased porosity and surface roughness. Contact angle study showed that nanotubes in the hydrogel increased the hydrophobicity of the gels. The cell viability tests confirm that the CH−CNT hybrid hydrogels (with 0.1% CNT) are biocompatible. An inclusion of 0.1% CNTs showed a high cell viability, but higher concentrations of CNTs reduced cell viability. Swelling behavior of the hybrid hydrogels was improved with CNT inclusion in the hydrogels. Swelling kinetics of the CH−CNT hybrid hydrogels was found to follow the Fickian behavior. Lysozyme digestion method was used to evaluate the in vitro degradation property of the hydrogels, and the result showed that nanotube inclusion lowered the degradation rate. However, a higher concentration of CNTs (0.5%) showed a higher degradation rate compared to a lower concentration of CNTs (0.1%). We also show that the CNT decreased the amount of cumulative release of MTX-loaded hydrogels compared with hydrogels without CNT. The CNT in the hydrogel allows a slower and more controllable release behavior of MTX. The antitumor effect of nanohybrid hydrogels on breast cancer cells shows that CH−β-GP−CNT hydrogels loaded with MTX could enhance the inhibition effect on MCF-7 breast cancer cell growth. The study suggests that the hybrid hydrogels of carbon nanomaterials and chitosan can function as injectable materials for the anticancer drug delivery such as MTX. The drug delivery system will contribute to the strategy of targeted therapy and sustainable chemotherapy.

4. MATERIALS AND METHODS

4.1. Preparation of Hydrogels. To prepare the thermosensitive CH−CNT hydrogels, chitosan (2.5%) and CNT (0, 0.1, 0.5, and 1%) were dissolved in acetic acid (0.05 M) using magnetic stirring for 12−24 h and then sonicated for 1 h. A solution of 40% (w/v) β-GP was also made in deionized water. The solutions were placed in a refrigerator for 15−30 min. Then, β-GP was added to the CH solution, mixed well at room temperature. Then, the mixture was transferred to an incubator of 37 °C, and hydrogel was formed after a few minutes. For all biological tests, the CH solutions were sterilized in an autoclave (121 °C, 20 min), and β-GP solutions were sterilized by filtration before they were used to form a hydrogel.

4.2. Chemical and Structural Analysis. The surface morphology of the prepared CH−CNT hydrogels was examined by scanning electron microscopy (Carl Zeiss Microscopy, LLC, Thornwood, NY). All lyophilized samples were lyophilized and coated with gold before the SEM test. To understand about how the addition of nanotubes affect the hydrophilicity of the prepared hydrogels, the static sessile drop method was performed to measure the surface water contact angle using a goniometer (CAM 100, KSV Instruments Ltd., Helsinki, Finland). A drop of Milli-Q water was placed on the film surface, and the shape of the droplet was recorded as a function of time with a FireWire connectable charge-coupled device camera with 50 mm optics.

To characterize the chemical structure of the CH−CNT hydrogels, FTIR spectra were obtained using a Nicolet FTIR spectrophotometer (Thermo Nicolet Avatar 360 FTIR). All spectra were within the range of 650−4000 cm^{-1} and recorded by a transmittance mode. An XploRATM PLUS Raman spectrometer (Horiba Scientific) was utilized to analyze the hydrogels at a wavelength of 100−3200 cm^{-1} using a 532 nm laser.

The phase and crystallinity of the prepared hydrogels were evaluated using X-ray diffraction. Measurements were performed using a fixed-anode X-ray generator (Rigaku, Geigerflex, 40 kV and 30 mA) with Cu Kα radiation (λ = 0.1542 nm) and 2θ ranging from 10 to 60°.

4.3. In Vitro Biological Analysis. The swelling test of the hydrogels was performed using the following method. The weight of the samples was measured and soaked in a phosphate buffer solution (PBS) (pH = 7) at 37 °C. At various time points, the weight of the samples was measured after the excess liquid was carefully wiped-off using filter papers. The swelling (SW) ratio was calculated using the following equation

$$\%\text{swelling ratio} = \frac{W_s - W_0}{W_0} \times 100$$

where W_0 represents the weight of the initial hydrogel and W_s is the weight of the wet hydrogel.

To investigate the biodegradability of the hydrogels, the weight of the samples was accurately measured and then placed in PBS for incubation at 37 °C in a shaking incubator. The hydrogel degradation rate was tested by adding lysozyme (0.02 mg/mL) into the PBS. At various time points, the hydrogels

DOI: 10.1021/acsomega.8b03212
ACS Omega 2019, 4, 4040−4048

were removed from the incubation medium and weighed. Weight reduction was determined by calculating the difference of the dry mass of the sample before and after incubation.

The alamarBlue assay (Pierce Biotechnology, Rockford, IL) was utilized to test the viability of cells grown on the CH−β-GP−CNT hydrogels. The hydrogels were prepared in the wells of a 24-well plate and then incubated at 37 °C for 2 h. The hydrogels were then seeded with 3T3 fibroblast cells, and the cells were cultured for 4 days. To perform the alamarBlue test, the reagent (10% v/v) was added to the cell culture well and incubated at 37 °C. After 4 h, the cell culture medium was transferred to a 96-well plate, and the absorbance of the medium was measured at 570 and 600 nm using a Synergy Mx Monochromator-Based Multi-Mode Microplate Reader (Winooski, VT). The samples with hydrogel alone were used as a control study. The cell viability was calculated according to the absorbance value.

The releasing profile of MTX from the MTX-loaded hydrogels into PBS was studied. The MTX was mixed with the CH−β-GP solution with various amounts of CNT (0, 0.1, and 0.5%) at room temperature. The hydrogel with MTX was formed after incubation of the solution in an incubator of 37 °C. The MTX-loaded hydrogels were immersed in the PBS solution, and the released MTX at various time intervals was measured. The cell culture medium (1 mL) was changed, collected, and the old medium was collected at each time point. The MTX level in the collected medium was tested using a UV−visible spectrophotometer (Hitachi-2900 Spectrophotometer) at 303 nm.

To study their antitumor efficiency of released MTX, the breast cancer cells (MCF-7) were grown on the MTX-loaded hydrogels. The antiproliferative effect of the released MTX on MCF-7 breast cancer cells was tested by the alamarBlue assay.

4.4. Statistical Analysis. The data are presented as mean ± standard deviation for $n = 3$ values. Statistical analysis was conducted using a two-tailed Student t-test. The p-value of less than 0.05 was considered as statistically significant.

AUTHOR INFORMATION

Corresponding Author

*E-mail: leylasaeednia@gmail.com.

ORCID

Leyla Saeednia: 0000-0002-5134-3375

Present Address

[‖]Pfizer Inc., 1776 Centennial Dr., McPherson, Kansas 67460, United States (L.S.).

Notes

The authors declare no competing financial interest.

ACKNOWLEDGMENTS

We would acknowledge Dr Andrew Swindle for his help on collecting XRD results. The authors are also grateful to Dr William J. Hendry, Professor and Chairman of the Department of Biological Sciences at Wichita State University, and Dr Fariba Behbod, Associate Professor at Division of Cancer and Developmental Biology at the University of Kansas, for their technical support. We acknowledge the National Institute of General Medical Sciences (P20 GM103418) of the National Institutes of Health for support of this study.

REFERENCES

(1) Mouawad, R.; Spano, J.-P.; Khayat, D. Lymphocyte infiltration in breast cancer: a key prognostic factor that should not be ignored. *J. Clin. Oncol.* **2011**, *29*, 1935−1936.

(2) Zhou, J.; Zhong, Y. Breast cancer immunotherapy. *Cell Mol. Immunol.* **2004**, *1*, 247−255.

(3) Ruel-Gariépy, E.; Shive, M.; Bichara, A.; Berrada, M.; Le Garrec, D.; Chenite, A.; Leroux, J.-C. A thermosensitive chitosan-based hydrogel for the local delivery of paclitaxel. *Eur. J. Pharm. Biopharm.* **2004**, *57*, 53−63.

(4) Ochekpe, N. A.; Olorunfemi, P. O.; Ngwuluka, N. C. Nanotechnology and drug delivery part 1: Background and applications. *Trop. J. Pharm. Res.* **2009**, *8*, 265−274.

(5) Martinho, N.; et al. Recent advances in drug delivery systems. *J. Biomater. Nanobiotechnol.* **2011**, *2*, 510−526.

(6) Peppas, N. A.; Hilt, J. Z.; Khademhosseini, A.; Langer, R. Hydrogels in biology and medicine: From molecular principles to bionanotechnology. *Adv. Mater.* **2006**, *18*, 1345−1360.

(7) Bhattarai, N.; Gunn, J.; Zhang, M. Chitosan-based hydrogels for controlled, localized drug delivery. *Adv. Drug Delivery Rev.* **2010**, *62*, 83−99.

(8) Ahmed, E. M. Hydrogel: Preparation, characterization, and applications. *J. Adv. Res.* **2013**, 105−121.

(9) Croisier, F.; Jérôme, C. Chitosan-based biomaterials for tissue engineering. *Eur. Polym. J.* **2013**, *49*, 780−792.

(10) Giri, T. K.; Thakur, A.; Alexander, A.; Badwaik, H.; Tripathi, D. K. Modified chitosan hydrogels as drug delivery and tissue engineering systems: Present status and applications. *Acta Pharm. Sin. B* **2012**, *2*, 439−449.

(11) Modrzejewska, Z.; Skwarczyńska, A.; Maniukiewicz, W.; Douglas, T. E. Mechanism of formation of thermosensitive chitosan chloride gels. *Prog. Chem. Appl. Chitin Deriv.* **2014**, *19*, 125−134.

(12) Kim, S.; Nishimoto, S. K.; Bumgardner, J. D.; Haggard, W. O.; Gaber, M. W.; Yang, Y. A chitosan/β-glycerophosphate thermosensitive gel for the delivery of ellagic acid for the treatment of brain cancer. *Biomaterials* **2010**, *31*, 4157−4166.

(13) Ghasemi Tahrir, F.; Ganji, F.; Mani, A. R.; Khodaverdi, E. In vitro and in vivo evaluation of thermosensitive chitosan hydrogel for sustained release of insulin. *Drug Delivery* **2014**, 1−9.

(14) Molinaro, G.; Leroux, J.-C.; Damas, J.; Adam, A. Biocompatibility of thermosensitive chitosan-based hydrogels: An in vivo experimental approach to injectable biomaterials. *Biomaterials* **2002**, *23*, 2717−2722.

(15) Yan, J.; Yang, L.; Wang, G.; Xiao, Y.; Zhang, B.; Qi, N. Biocompatibility evaluation of chitosan-based injectable hydrogels for the culturing mice mesenchymal stem cells in vitro. *J. Biomater. Appl.* **2010**, *24*, 625−637.

(16) Ngoenkam, J.; Faikrua, A.; Yasothornsrikul, S.; Viyoch, J. Potential of an injectable chitosan/starch/β-glycerol phosphate hydrogel for sustaining normal chondrocyte function. *Int. J. Pharm.* **2010**, *391*, 115−124.

(17) Satarkar, N. S.; Johnson, D.; Marrs, B.; Andrews, R.; Poh, C.; Gharaibeh, B.; Saito, K.; Anderson, K. W.; Hilt, J. Z. Hydrogel-MWCNT nanocomposites: Synthesis, characterization, and heating with radiofrequency fields. *J. Appl. Polym. Sci.* **2010**, *117*, 1813−1819.

(18) Lovinger, A. J. Nano-, Bio-, Multi-, Inter-,...: Polymer Research in an Era of Prefixes. *J. Macromol. Sci., Part C: Polym. Rev.* **2005**, *45*, 195−199.

(19) Zhang, X.; Pint, C. L.; Lee, M. H.; Schubert, B. E.; Jamshidi, A.; Takei, K.; Ko, H.; Gillies, A.; Bardhan, R.; Urban, J. J.; et al. Optically- and thermally-responsive programmable materials based on carbon nanotube-hydrogel polymer composites. *Nano Lett.* **2011**, *11*, 3239−3244.

(20) Tong, X.; Zheng, J.; Lu, Y.; Zhang, Z.; Cheng, H. Swelling and mechanical behaviors of carbon nanotube/poly(vinyl alcohol) hybrid hydrogels. *Mater. Lett.* **2007**, *61*, 1704−1706.

(21) Liu, Z.; Sun, X.; Nakayama-Ratchford, N.; Dai, H. Supramolecular chemistry on water-soluble carbon nanotubes for drug loading and delivery. *ACS Nano* **2007**, *1*, 50−56.

DOI: 10.1021/acsomega.8b03212
ACS Omega 2019, 4, 4040−4048

(22) Kam, N. W. S.; Dai, H. Carbon nanotubes as intracellular protein transporters: generality and biological functionality. *J. Am. Chem. Soc.* **2005**, *127*, 6021−6026.
(23) Hussain, M.; Kabir, M.; Sood, A. On the cytotoxicity of carbon nanotubes. *Curr. Sci.* **2009**, *96*, 664−673.
(24) Ezzati Nazhad Dolatabadi, J.; Omidi, Y.; Losic, D. Carbon nanotubes as an advanced drug and gene delivery nanosystem. *Curr. Nanosci.* **2011**, *7*, 297−314.
(25) Cirillo, G.; Hampel, S.; Spizzirri, U. G.; Parisi, O. I.; Picci, N.; Iemma, F. Carbon nanotubes hybrid hydrogels in drug delivery: A perspective review. *BioMed Res. Int.* **2014**, *2014*, 1−18.
(26) Chatterjee, S.; Lee, M. W.; Woo, S. H. Enhanced mechanical strength of chitosan hydrogel beads by impregnation with carbon nanotubes. *Carbon* **2009**, *47*, 2933−2936.
(27) Li, H.; Wang, D.; Liu, B.; Gao, L. Synthesis of a novel gelatin−carbon nanotubes hybrid hydrogel. *Colloids Surf., B* **2004**, *33*, 85−88.
(28) Ferris, C. J. Conducting bio-materials based on gellan gum hydrogels. *Soft Matter* **2009**, *5*, 3430−3437.
(29) Rodrigues, A. A.; Batista, N. A.; Bavaresco, V. P.; Baranauskas, V.; Ceragioli, H. J.; Peterlevitz, A. C.; Mariolani, J. R.; Santana, M. H.; Belangero, W. D. In vivo evaluation of hydrogels of poly(vinyl alcohol) with and without carbon nanoparticles for osteochondral repair. *Carbon* **2012**, *50*, 2091−2099.
(30) Venkatesan, J.; Ryu, B.; Sudha, P.; Kim, S.-K. Preparation and characterization of chitosan−carbon nanotube scaffolds for bone tissue engineering. *Int. J. Biol. Macromol.* **2012**, *50*, 393−402.
(31) Aryaei, A.; Jayatissa, A. H.; Jayasuriya, A. C. Mechanical and biological properties of chitosan/carbon nanotube nanocomposite films. *J. Biomed. Mater. Res., Part A* **2014**, *102*, 2704−2712.
(32) Ganji, F.; Vasheghani-Farahani, E. Hydrogels in controlled drug delivery systems. *Iran. Polym. J.* **2009**, *18*, 63−88.
(33) Ahuja, G.; Pathak, K. Porous carriers for controlled/modulated drug delivery. *Indian J. Pharm. Sci.* **2009**, *71*, 599−607.
(34) Hoare, T. R.; Kohane, D. S. Hydrogels in drug delivery: Progress and challenges. *Polymer* **2008**, *49*, 1993−2007.
(35) Lotfi, M.; Naceur, M.; Nejib, M. *Cell Adhesion to Biomaterials: Concept of Biocompatibility, Advances in Biomaterials Science and Biomedical Applications*; INTECH Open Access Publisher, 2013.
(36) Katalinich, M. *Characterization of Chitosan Films for Cell Culture Applications*; The University of Maine, 2001.
(37) Shin, Y. J.; Wang, Y.; Huang, H.; Kalon, G.; Wee, A. T. S.; Shen, Z.; Bhatia, C. S.; Yang, H. Surface-energy engineering of graphene. *Langmuir* **2010**, *26*, 3798−3802.
(38) Aldalbahi, A.; in het Panhuis, M. Electrical and mechanical characteristics of buckypapers and evaporative cast films prepared using single and multi-walled carbon nanotubes and the biopolymer carrageenan. *Carbon* **2012**, *50*, 1197−1208.
(39) Tajima, Y.; Matsuura, T.; Numata, Y.; Yamazaki, D.; Kawamura, H.; Osedo, H. Surface free energy and wettability determination of various fullerene derivative films on amorphous carbon wafer. *Jpn. J. Appl. Phys.* **2008**, *47*, 5730−5733.
(40) Venkatesan, J.; Jayakumar, R.; Mohandas, A.; Bhatnagar, I.; Kim, S.-K. Antimicrobial activity of chitosan-carbon nanotube hydrogels. *Materials* **2014**, *7*, 3946−3955.
(41) Yang, S.; Shao, D.; Wang, X.; Hou, G.; Nagatsu, M.; Tan, X.; Ren, X.; Yu, J. Design of chitosan-grafted carbon nanotubes: evaluation of How the −OH functional group affects Cs+ adsorption. *Mar. Drugs* **2015**, *13*, 3116−3131.
(42) Hodkiewicz, J. *Characterizing Carbon Materials with Raman Spectroscopy*; Thermo Scientific, Application Note 51901, 2010.
(43) Kim, D. S.; Dhand, V.; Rhee, K. Y.; Park, S.-J. Study on the effect of silanization and improvement in the tensile behavior of graphene-chitosan-composite. *Polymers* **2015**, *7*, 527−551.
(44) Sayyar, S.; Murray, E.; Thompson, B.; Chung, J.; Officer, D. L.; Gambhir, S.; Spinks, G. M.; Wallace, G. G. Processable conducting graphene/chitosan hydrogels for tissue engineering. *J. Mater. Chem. B* **2015**, *3*, 481−490.
(45) Chen, M.-L.; Oh, W.-C. Synthesis and highly visible-induced photocatalytic activity of CNT-CdSe composite for methylene blue solution. *Nanoscale Res. Lett.* **2011**, *6*, 1−8.
(46) Jiang, R.; Zhu, H.; Yao, J.; Fu, Y.; Guan, Y. Chitosan hydrogel films as a template for mild biosynthesis of CdS quantum dots with highly efficient photocatalytic activity. *Appl. Surf. Sci.* **2012**, *258*, 3513−3518.
(47) Yasmeen, S.; Lo, M. K.; Bajracharya, S.; Roldo, M. Injectable scaffolds for bone regeneration. *Langmuir* **2014**, *30*, 12977−12985.
(48) Wang, S.-F.; Shen, L.; Zhang, W.-D.; Tong, Y.-J. Preparation and mechanical properties of chitosan/carbon nanotubes composites. *Biomacromolecules* **2005**, *6*, 3067−3072.
(49) Ta, H. T.; Dass, C. R.; Dunstan, D. E. Injectable chitosan hydrogels for localised cancer therapy. *J. Controlled Release* **2008**, *126*, 205−216.
(50) Nwe, N.; Furuike, T.; Tamura, H. The mechanical and biological properties of chitosan scaffolds for tissue regeneration templates are significantly enhanced by chitosan from Gongronella butleri. *Materials* **2009**, *2*, 374−398.
(51) Dash, S.; Murthy, P. N.; Nath, L.; Chowdhury, P. Kinetic modeling on drug release from controlled drug delivery systems. *Acta Pol. Pharm.* **2010**, *67*, 217−223.
(52) Niranjan, R.; Koushik, C.; Saravanan, S.; Moorthi, A.; Vairamani, M.; Selvamurugan, N. A novel injectable temperature-sensitive zinc doped chitosan/β-glycerophosphate hydrogel for bone tissue engineering. *Int. J. Biol. Macromol.* **2013**, *54*, 24−29.
(53) Peng, Q.; Sun, X.; Gong, T.; Wu, C.-Y.; Zhang, T.; Tan, J.; Zhang, Z.-R. Injectable and biodegradable thermosensitive hydrogels loaded with PHBHHx nanoparticles for the sustained and controlled release of insulin. *Acta Biomater.* **2013**, *9*, 5063−5069.
(54) Gorgieva, S.; Kokol, V. Preparation, characterization, and in vitro enzymatic degradation of chitosan-gelatine hydrogel scaffolds as potential biomaterials. *J. Biomed. Mater. Res., Part A* **2012**, *100*, 1655−1667.
(55) Markaki, A. *alamarBlue Assay for Assessment of Cell Proliferation using the FLUOstar OPTIMA*; BMG Lab Tech, 2009.
(56) Pandey, H.; Parashar, V.; Parashar, R.; Prakash, R.; Ramteke, P. W.; Pandey, A. C. Controlled drug release characteristics and enhanced antibacterial effect of graphene nanosheets containing gentamicin sulfate. *Nanoscale* **2011**, *3*, 4104−4108.
(57) Korsmeyer, R. W.; Gurny, R.; Doelker, E.; Buri, P.; Peppas, N. A. Mechanisms of solute release from porous hydrophilic polymers. *Int. J. Pharm.* **1983**, *15*, 25−35.

DOI: 10.1021/acsomega.8b03212
ACS Omega 2019, 4, 4040−4048